

## Role of the Range in the Fluid–Crystal Coexistence for a Patchy Particle Model

Flavio Romano,<sup>\*,†</sup> Eduardo Sanz,<sup>‡</sup> and Francesco Sciortino<sup>†</sup>

Dipartimento di Fisica and INFN-CNR-SOFT, Università di Roma La Sapienza, Piazzale A. Moro 2, 00185 Roma, Italy, and SUPA, School of Physics and Astronomy, University of Edinburgh, Mayfield Road, Edinburgh, U.K.

Received: August 25, 2009; Revised Manuscript Received: September 24, 2009

We evaluate the phase diagram of the four-site Kern–Frenkel patchy particle model [Kern, N.; Frenkel, D. *J. Chem. Phys.* **2003**, *118*, 9882.], a model representative of particles interacting via short-range orientational interactions, for several values of the interaction range. Similar to what has been found for isotropic potentials, the liquid phase disappears as an equilibrium phase for values of the range on the order of 15% of the particle diameter. For smaller ranges, the gas–liquid phase separation becomes metastable with respect to crystallization into a diamond-like structure. Interestingly, and differently from the isotropic case, the supersaturation of the fluid at the critical point does not significantly increase upon going toward the adhesive (vanishing interaction range) limit.

By contrast with atoms or molecules, micro- and nanosized colloidal particles can interact with ranges significantly smaller than their size, giving rise to novel and intriguing physical phenomena unseen in molecular systems. A remarkable example is the disappearance of the liquid from the equilibrium phase diagram for attractive ranges smaller than roughly a fourth of the particle diameter,<sup>1–3</sup> the exact threshold being slightly dependent on the specific shape of the potential.<sup>1,4,5</sup> This is a very important finding since the formation of certain types of colloidal gels<sup>6</sup> as well as the behavior of some globular proteins<sup>7</sup> can be accounted for by the presence of a metastable gas–liquid coexistence. Proteins, in particular, have triggered many studies of the phase behavior of short-ranged interacting systems, many of them motivated by the need for some guidance in the arduous process of crystallizing these macromolecules,<sup>8,9</sup> required to elucidate their structure via X-ray diffraction.<sup>10–13</sup> ten Wolde and Frenkel have shown that crystallization is significantly enhanced for quenches to the metastable critical point as critical density fluctuations increase the chance to form solid nuclei.<sup>8</sup> However, density fluctuations alone do not guarantee crystal formation since a large driving force for crystallization is also required. The so-called metastability gap,<sup>4</sup>  $M$ , is a measure of the degree of metastability, that is, of the driving force for crystal nucleation, at the critical point

$$M \equiv \frac{(T_x - T_c)}{T_c} \quad (1)$$

where  $T_c$  is the metastable critical temperature and  $T_x$  the freezing temperature at the critical density. For isotropic, short-ranged, attractive potentials, like the one used by ten Wolde and Frenkel as a simple protein model,<sup>8</sup> both  $T_c$  and  $T_x$  decrease

upon decreasing the interaction range. The former, however, does it to a major extent,<sup>4</sup> resulting in an increase of  $M$  as the range narrows, which makes crystallization at the critical point possible.

While the picture for isotropic potentials seems rather complete, much less is known about the case of short-ranged, anisotropic, patchy potentials, that is, potentials characterized by interacting sites localized on the surface of the particle. Patchy interactions may impose a precise constraint on the maximum number of bonded neighbors, which we will refer to as valence. A number of reasons have triggered a great interest in understanding the phase behavior of patchy particles,<sup>14,15</sup> among we name that (i) the phase behavior of some proteins is believed to depend crucially on the directionality of the interactions;<sup>16,17</sup> (ii) the self-assembly of patchy particles into target structures can be achieved by tailoring the geometry of the interacting sites;<sup>18</sup> and (iii) patchy interactions provide new insights into the physics of arrested dynamics.<sup>19</sup> Moreover, state-of-the-art techniques of colloidal syntheses have proved able to engineer particles with patchy interactions.<sup>18</sup>

An interesting case is that of low-valence patchy interactions. Although the gas–liquid coexistence has already been investigated for valences three, four, and five,<sup>20</sup> there are intriguing open questions regarding the liquid–solid competition. In particular, Charbonneau and Frenkel have recently put forward the possibility of the existence of a critical valence below which the liquid retains its thermodynamic stability down to the vanishing range limit.<sup>21</sup> Were this the case, the crystallization route proposed by ten Wolde and Frenkel<sup>8</sup> would not be effective, with important implications for protein crystallization and self-assembly of patchy colloidal particles.

In this Letter, we investigate numerically the fluid–crystal and gas–liquid coexistence curves for tetrahedrally coordinated particles, modeled via the Kern–Frenkel (KF) potential<sup>22</sup> for values of the interaction range comprised between 24 and 3% of the particle diameter. As in the spherical case, we find that

\* To whom correspondence should be addressed.

† Università di Roma.

‡ University of Edinburgh.

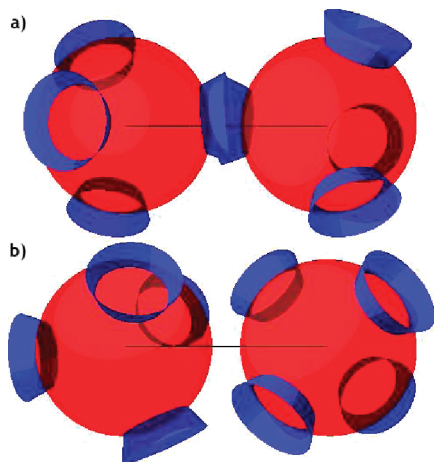


**Figure 1.** Cartoon of two patchy particles in a bonded (a) and not bonded (b) configuration. The four interaction sites are arranged on a regular tetrahedron inscribed in a hard sphere of diameter  $\sigma$ . The attractive regions are represented by cones of semiangle  $\theta_{\max}$ . Particles are bonded with energy  $-u_0$  when their center-to-center distance is less than  $\sigma + \Delta$  and the vector connecting the two particle centers (dark line in the picture) passes through any two cones.

upon reducing the interaction range, the liquid ceases to exist as an equilibrium phase. This happens at a lower range, that is, around  $\Delta \approx 0.15$  as opposed to  $\Delta \approx 0.25$  of the spherical case. However, in contrast with the isotropic case, the metastability gap, as well as the difference in chemical potential between the liquid and the crystal phases, does not significantly grow upon shrinking the range.

The KF model, properly defined in ref 22, envisages a particle as a hard sphere of diameter  $\sigma$  whose surface is decorated by interacting sites, in our case four in a tetrahedral arrangement. Two sites,  $i$  and  $j$ , belonging to two different particles  $a$  and  $b$ , respectively, interact with energy  $-u_0$  if the following two conditions are fulfilled: (i) the distance between the particles' centers is smaller than  $\sigma + \Delta$  and (ii) both angles site $_i$ -center $_a$ -center $_b$  and site $_j$ -center $_b$ -center $_a$  are smaller than  $\theta_{\max}$ . A pictorial representation of a bonded and a nonbonded configuration is provided in Figure 1. We studied the thermodynamic behavior of this model for  $\cos(\theta_{\max}) = 0.92$  and for five different values of  $\Delta/\sigma = 0.03, 0.07, 0.12, 0.18$ , and  $0.24$ . This set of parameters obeys the inequality  $\sin(\theta_{\max}) \leq [2(1 + \Delta/\sigma)]^{-1}$ , which ensures that no interacting site is involved in more than one bond.<sup>20</sup> We use reduced units with  $\sigma = 1$  and  $u_0 = 1$ , temperature  $T$  measured in units of  $u_0$  (Boltzmann constant  $k_B = 1$ ), number density  $\rho$  in units of  $\sigma^{-3}$ , and pressure  $P$  in units of  $u_0/\sigma^3$ .

We follow the guidelines reviewed in the recent article by Vega et al.<sup>23</sup> to calculate the fluid and solid free energies and to trace the associated coexistence lines. To compute the free energy of the fluid, we use thermodynamic integration along an isotherm starting from the low-density (ideal gas) limit. The free energy of the solid phases is computed via the Frenkel-Ladd method,<sup>24</sup> extended to anisotropic potentials as described in ref 23. Finite size corrections to the free energy are taken into account.<sup>25</sup> The gas-liquid coexistence lines are calculated via the Gibbs ensemble Monte Carlo technique.<sup>26</sup> Critical parameters are either taken from ref 20 or calculated as described therein ( $\Delta = 0.18$  and  $0.24$ ). Fluid-solid coexistence lines are calculated via the Gibbs-Duhem integration technique introduced by Kofke.<sup>27</sup>

Three kinds of consistency checks were performed to make sure our simulation and integration scheme yields reliable

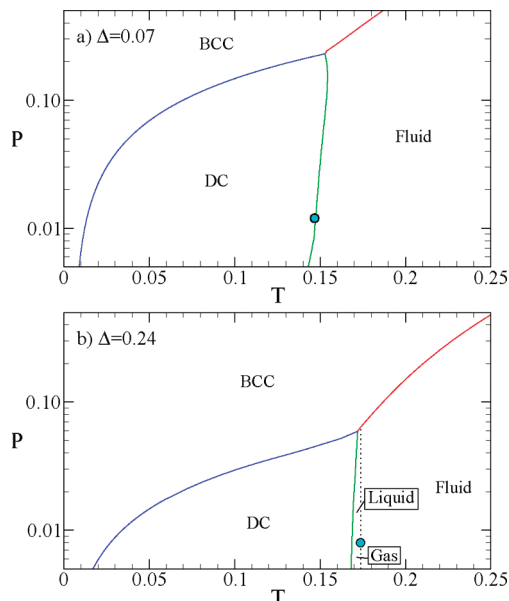


**Figure 2.** Phase diagrams of the four-patch KF model in the ( $p$ - $T$ ) plane with  $\Delta = 0.07$  (a) and  $0.24$  (b). In the first case, the gas-liquid critical point from ref 20 (filled circle) is metastable. Reduced units are defined in the text. Note the logarithmic scale of the pressures. The distinction between fluid, gas, and liquid is made evident via the dotted line.

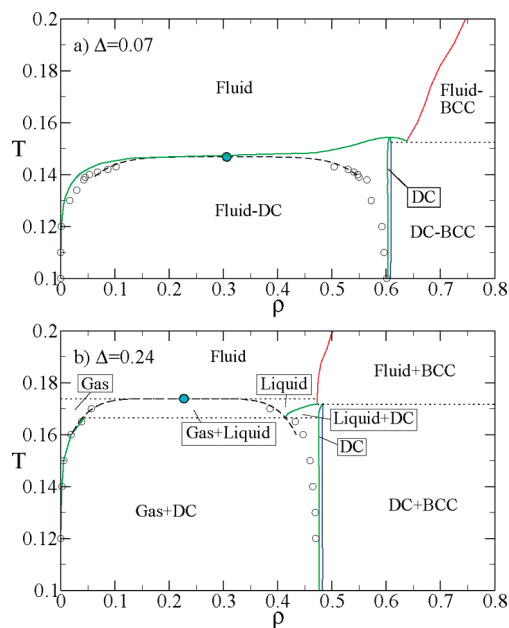


**Figure 3.** Phase diagrams in the ( $T$ - $\rho$ ) plane. Only in (a) the gas-liquid coexistence line is metastable with respect to crystallization to the DC phase. Open circles represent gas-liquid coexistence results, while filled circles represent the critical points. Solid lines mark the coexistence density of each phase at a given temperature, while dotted lines mark the borders between different regions of the phase diagram. Dashed lines are fits to the Gibbs ensemble simulation data according to  $(\rho \pm \rho_c) = A|T - T_c| \pm B|T - T_c|^b$  with  $b = 0.3258$ . Labels outside of their regions are framed.

results;<sup>23</sup> the free energy of the fluid phase was double-checked with Grand Canonical Monte Carlo simulations; the direct coexistence method<sup>28</sup> was used to check fluid-solid coexistence points; and Hamiltonian Gibbs-Duhem integration was used to check the displacement with  $\Delta$  of the coexistence lines. More detailed information on the numerical techniques will be reported in a future publication.<sup>29</sup>

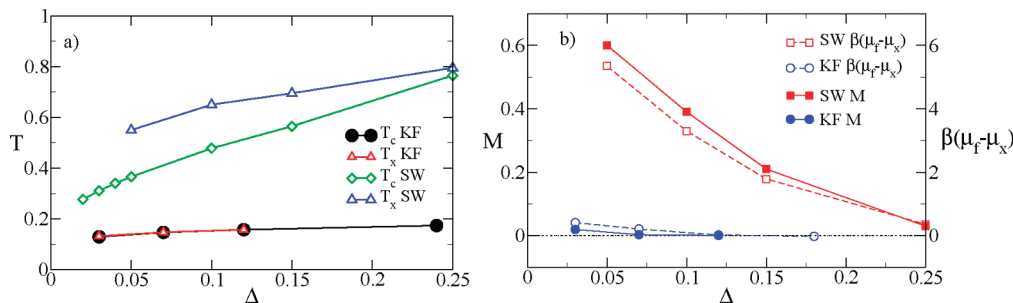


**Figure 4.** (a)  $\Delta$  dependence of  $T_c$  and  $T_x$  at  $\rho_c$  for the SW and KF models. SW critical points are taken from ref 31.  $T_x$  values are either taken from ref 4 ( $\Delta = 0.25, 0.15$ ) or evaluated here via direct coexistence ( $\Delta = 0.10, 0.05$ ). (b) Metastability gap (filled symbols) and difference in chemical potential (open symbols) for the SW (squares) and KF (circles) versus the interaction range  $\Delta$ . The lines start from the first studied  $\Delta$  with a metastable gas–liquid coexistence since  $M$  cannot be defined when the liquid phase is thermodynamically stable. Errors on  $M$  can arise from finite-size effects ( $T_c$ ) and the Frenkel–Ladd procedure ( $T_x$ ) and are smaller than the symbol size.<sup>3,20</sup> Errors on  $\beta(\mu_c - \mu_x)$  can be estimated as less than 0.04,<sup>3,23</sup> also smaller than the symbol size in the figure.

We have considered two representative crystal structures, the diamond cubic (DC) and the body-centered cubic (BCC) crystals. Both of these structures are characterized by tetrahedrally ordered arrangements of fully bonded particles. The DC is an open crystal structure, while the BCC is a dense crystal constituted by two interpenetrating tetrahedrally bonded lattices (its density is approximately twice as large as that of DC). With the present choice of  $\theta_{\max}$ , a face-centered cubic (FCC) crystal has also an energy per particle of  $-2\mu_0$  (i.e., all four sites of every particle are involved in a bond), but bonded neighbors are not tetrahedrally oriented, significantly diminishing the angular phase space available to the bonded crystal. As a result, in the region of the phase diagram in which we are interested, the proximity of the gas–liquid coexistence, the FCC free energy is always higher than that of BCC or DC. We do not investigate the high- $T$  region, where the phase diagram will tend to that of hard spheres, with a stable fluid and a plastic FCC crystal.<sup>14</sup>

Two of the four investigated phase diagrams are reported in Figure 2 ( $\rho$ – $T$  plane) and in Figure 3 ( $T$ – $\rho$  plane). At  $\Delta = 0.18$  and 0.24, the liquid phase is stable, while at  $\Delta = 0.12$  and smaller values, the gas–liquid coexistence is preempted by the DC–fluid coexistence line. Hence, the liquid ceases to exist as an equilibrium phase at  $\Delta = 0.15 \pm 0.03$ , as opposed to  $\Delta \approx 0.25$  found for the SW potential. For densities around  $\rho_c$ , the fluid–DC freezing curve is almost flat in the  $T$ – $\rho$  plane, analogous to the top part of the gas–liquid coexistence curve. The stability region of the DC in the ( $\rho$ – $T$ ) plane is very narrow due to the short-range nature of the potential, which limits the maximum distance over which particles can form bonds. For all investigated  $\Delta$ , the competition between the liquid and the crystal involves the DC structure. The BCC is indeed found to be stable only at  $p \gg p_c$ . Decreasing the range destabilizes the BCC crystal with respect to both the fluid and DC. In the ( $T$ – $\rho$ ) plane, the stability regions of the crystals shrink as  $\Delta$  decreases. This is due to the fact that, for short ranges, particles barely move away from their lattice positions in order to remain bonded.

The competition between solid and liquid can be assessed by means of the metastability gap ( $M$  in eq 1); the larger the gap, the more stable the solid with respect to the liquid at the critical point. First, we show in Figure 4a the  $\Delta$  dependence of  $T_x$  and  $T_c$  for both the SW potential and the KF model. The solid structures competing with the liquid are FCC and DC for SW and KF, respectively. For the SW case, the fluid–crystal coexistence curve had not been previously calculated for very small  $\Delta$ ; we have therefore evaluated  $T_x$  ourselves for both  $\Delta$

$= 0.05$  and 0.10 using the direct coexistence method. Interestingly enough, while for the SW potential,  $T_x$  decreases much slower than  $T_c$  upon lowering  $\Delta$  for the patchy case  $T_x$  closely tracks  $T_c$ . The difference between the two potentials is more clearly seen in  $M$ , shown in Figure 4b. While for the SW potential  $M$  significantly increases upon decreasing  $\Delta$ , it does it only slightly for the tetrahedral KF model, remaining close to zero in the entire range of  $\Delta$  explored.

Figure 4b clearly shows that, for tetrahedrally interacting particles, the metastability gap does not significantly increase as the interaction range decreases. To strengthen this observation, we also evaluate and report in the same figure the difference between the reduced chemical potentials of the fluid and the crystal  $\beta(\mu_f - \mu_x)$  at the gas–liquid critical  $T$  and pressure. The calculated small values confirm that no significant driving force for crystallization is present. Moreover, as noted above, the fluid–crystal freezing curve is rather flat in ( $T$ – $\rho$ ) around  $\rho_c$ . Doing thermodynamic integration from the critical point, we estimate that a density fluctuation leading to a fluid with  $\rho = 2\rho_c$  only increases  $\beta(\mu_f - \mu_x)$  by roughly 0.1. Therefore, particles interacting through tetrahedrally arranged patches are not expected to crystallize at higher rates close to the critical point. Indeed, we have never observed crystallization in our lengthy simulations of the model. This is in contrast with the spherically interacting case, where sitting close to the critical point does favor crystallization both because  $\beta(\mu_f - \mu_x)$  (whose calculated values are shown in Figure 4b) is about 10 times larger than the anisotropic case and because critical density fluctuations enhance the probability of forming a crystal nucleus.<sup>8</sup> This suggests that fairly high crystallization rates for small-valence interacting particles can be expected only well inside of the metastable gas–liquid coexistence. On the other hand, while a deep quench does generate a large  $\beta(\mu_f - \mu_x)$ , it may well bring the system in a state where, due to the small  $T$ , kinetic traps significantly slow down the formation of an ordered crystal phase.

Recent experiments have provided convincing evidence that in proteins, nucleation rates can be exquisitely sensitive to the degree of anisotropy.<sup>17</sup> Our results, although based on a specific tetra-functional model which crystallizes in a DC structure (not found experimentally among proteins<sup>30</sup>), can provide a starting point, which needs to be complemented by investigations of models with different valences, for disentangling the role of the range and the role of the patchiness, thus deepening our understanding of protein crystallization.

Results shown in Figure 4b also raise the interesting question of the possibility of a stabilization of the liquid phase

upon decreasing the valence. While definitive studies will require the estimate of the metastability gap for different valences (we plan to investigate this effect in the near future), the observed small  $\Delta$  dependence of  $M$  does suggest that it could exist a critical valence (smaller than four), below which the liquid retains its thermodynamic stability down to the vanishing range limit.<sup>21</sup>

**Acknowledgment.** We acknowledge support from NoE SoftComp NMP3-CT-2004-502235 and ERC-226207-PATCHYCOLLOIDS. E.S. thanks U.K. EPSRC EP/E030173/1 for financial support and the people of La Sapienza for their hospitality. We thank J. Bergholtz, P. Tartaglia, J. Russo, and P. G. De Sanctis Lucentini for interesting discussions.

## References and Notes

- (1) Hagen, M. H. J.; Frenkel, D. *J. Chem. Phys.* **1994**, *101*, 4093.
- (2) Ilett, S. M.; Orrock, A.; Poon, W. C. K.; Pusey, P. N. *Phys. Rev. E* **1995**, *51*, 1344.
- (3) Romano, F.; Tartaglia, P.; Sciortino, F. *J. Phys.: Condens. Matter* **2007**, *19*, 322101–322122.
- (4) Pagan, D. L.; Gunton, J. D. *J. Chem. Phys.* **2005**, *122*, 184515.
- (5) Liu, H.; Garde, S.; Kumar, S. *J. Chem. Phys.* **2005**, *123*, 174505.
- (6) Lu, P. J.; Zaccarelli, E.; Ciulla, F.; Schofield, A. B.; Sciortino, F.; Weitz, D. A. *Nature* **2008**, *453*, 06931.
- (7) Asherie, N.; Lomakin, A.; Benedek, G. B. *Phys. Rev. Lett.* **1996**, *77*, 4832–4835.
- (8) ten Wolde, P. R.; Frenkel, D. *Science* **1997**, *277*, 1975.
- (9) Dixit, N. M.; Zukosky, C. F. *J. Colloid Interface Sci.* **2000**, *228*, 359–371.
- (10) McPherson, A. *Preparation and Analysis of Protein Crystals*; Krieger: Malabar, FL, 1982.
- (11) Derewenda, Z. S.; Vekilov, P. G. *Acta Crystallogr.* **2006**, *D62*, 116–124.
- (12) Gunton, J. D.; Shiriyayev, A.; Pagan, D. L. *Protein Crystallization*; Cambridge University Press: New York, 2007.
- (13) Sear, R. P. *J. Phys.: Condens. Matter* **2007**, *19*, 033101.
- (14) Noya, E. G.; Vega, C.; Doye, J. P. K.; Louis, A. A. *J. Chem. Phys.* **2007**, *127*, 054501.
- (15) Wilber, A. W.; Doye, J. P. K.; Louis, A. A.; Noya, E. G.; Miller, M. A.; Wong, P. *J. Chem. Phys.* **2007**, *127*, 085106.
- (16) Pellicane, G.; Smith, G.; Sarkisov, L. *Phys. Rev. Lett.* **2008**, *101*, 248102.
- (17) McManus, J. J.; Lomakin, A.; Ogun, O.; Pande, A.; Basan, M.; Pande, J.; Benedek, G. B. *Proc. Natl. Acad. Sci.* **2007**, *104*, 16856–16861.
- (18) Glotzer, S. C.; Solomon, M. J. *Nat. Mater.* **2005**, *6*, 557–562.
- (19) Zaccarelli, E.; Buldyrev, S.; Nave, E. L.; Moreno, A. J.; Saika-Voivod, I.; Sciortino, F.; Tartaglia, P. *Phys. Rev. Lett.* **2005**, *94*, 218301.
- (20) Foffi, G.; Sciortino, F. *J. Phys. Chem. B* **2007**, *33*, 9702–9705.
- (21) Charbonneau, P.; Frenkel, D. *J. Chem. Phys.* **2007**, *126*, 054501.
- (22) Kern, N.; Frenkel, D. *J. Chem. Phys.* **2003**, *118*, 9882–9889.
- (23) Vega, C.; Sanz, E.; Abascal, J. L. F.; Noya, E. G. *J. Phys.: Condens. Matter* **2008**, *20*, 153101–153139.
- (24) Frenkel, D.; Ladd, A. J. C. *J. Chem. Phys.* **1984**, *81*, 3188.
- (25) Polson, J. M.; Trizac, E.; Pronk, S.; Frenkel, D. *J. Chem. Phys.* **2000**, *112*, 5339.
- (26) Panagiotopoulos, A. Z. *Mol. Phys.* **1987**, *61*, 813–826.
- (27) Kofke, D. A. *Mol. Phys.* **1993**, *78*, 1331–1336.
- (28) Ladd, A. J. C.; Woodcock, L. *Chem. Phys. Lett.* **1977**, *51*, 155–159.
- (29) Romano, F.; et al. In preparation.
- (30) Wukovitz, S. W.; Yeates, T. O. *Nat. Struct. Biol.* **1995**, *2*, 1062–1067.
- (31) Largo, J.; Miller, M. A.; Sciortino, F. *J. Chem. Phys.* **2003**, *128*, 134513.

JP9081905